

**Climatology, seasonality and trends of oceanic coherent
eddies**

Josué Martínez-Moreno¹, Andrew McC. Hogg¹, and Matthew England²

⁴ Research School of Earth Science and ARC Center of Excellence for Climate Extremes, Australian
⁵ National University, Canberra, Australia

⁶ Climate Change Research Centre (CCRC), UNSW Australia, Sydney NSW, Australia

Key Points:

- ⁸ Kinetic energy of coherent eddies contain around 30% of the surface ocean kinetic
⁹ energy budget.
- ¹⁰ Seasonal cycle of the number of coherent eddies and coherent eddy amplitude re-
¹¹ veal a 3-6 month lag to wind forcing
- ¹² The coherent eddy amplitude has increase at a rate of 3 cm per decade since 1993.

13 Abstract

Ocean eddies influence regional and global climate through mixing and transport of heat and properties. One of the most recognizable and ubiquitous feature of oceanic eddies are vortices with spatial scales of tens to hundreds of kilometers, frequently referred as “mesoscale eddies” or “coherent eddies”. Coherent eddies are known to transport properties across the ocean and to locally affect near-surface wind, cloud properties and rainfall patterns. Although coherent eddies are ubiquitous, yet their climatology, seasonality and long-term temporal evolution remains poorly understood. Thus, we examine the kinetic energy contained by coherent eddies and we present the annual, interannual, and long-term changes of automatically identified coherent eddies from satellite observations and a state of the art numerical simulation from 1993 to 2018. Satellite observations show that around 40% of the kinetic energy contained by ocean eddies corresponds to coherent eddies. Additionally, a strong hemispherical seasonal cycle is observed, on top of a 3–6 months lag between the wind forcing and the response of the coherent eddy field. Furthermore, the seasonality of the number of coherent eddies and their amplitude reveals that the number of coherent eddies responds faster to the forcing (~ 3 months), while the coherent eddy amplitude is lagged by ~ 6 months. There are regions that show a pronounced influence of coherent eddies, notably, the East Indian Ocean, the East Tropical Pacific Ocean, and the South Atlantic Ocean. In these locations, a strong seasonal cycle and interannual variability can be observed in both satellite and numerical models. Although, there is agreement between these products on the seasonality of the number of eddies, the seasonality of the coherent eddy amplitude between these products show some inconsistencies. Long-term trends of the coherent eddy amplitude from satellite observations and the state of the art model show significant increases in the eddy amplitude of $\sim 3\text{cm}$ per decade in large portions of the ocean, while the number of coherent eddies remains constant. Our analysis highlight the relative importance of the coherent eddy fiend in the ocean kinetic energy budget, imply a strong response of the eddy number and eddy amplitude to the surface wind at different time-scales, and showcases for the first time seasonality, and multidecadal trends of the coherent eddy properties.

42 Plain language summary

43 1 Introduction

44 Mesoscale ocean variability with spatial scales of tens to hundreds of kilometers is
 45 comprised by processes such as vortices, waves, and jets (Ferrari & Wunsch, 2009; Fu
 46 et al., 2010). These mesoscale processes are highly energetic, and they play a crucial role
 47 in the transport of heat, salt, momentum and other tracers through the ocean (Wunsch
 48 & Ferrari, 2004; Wyrtki et al., 1976; Gill et al., 1974). Possibly, the most recognizable
 49 and abundant process observed from satellites are mesoscale vortices. Although mesoscale
 50 vortices are commonly refer in literature as “mesoscale eddies”, this term is also often
 51 used to describe mesoscale ocean variability (time-varying component of flow), thus, here
 52 we will refer to mesoscale vortices as coherent eddies.

53 Coherent eddies are circular currents and according to their rotational direction,
 54 the sea surface height anomaly within a coherent eddy can have a negative or positive
 55 sea surface height anomaly (cold core and warm core coherent eddies, respectively). This
 56 characteristic sea surface height signature of coherent eddies has been utilized to auto-
 57 matically identified and tracked coherent eddies from satellite altimetry (Cui et al., 2020;
 58 Martínez-Moreno et al., 2019; Ashkezari et al., 2016; Faghmous et al., 2015; Chelton et
 59 al., 2007). Automated identification algorithms of coherent eddies have shown their ubiq-
 60 uity in the oceans, with a predominant influence at hotspots of eddy activity such as bound-
 61 ary currents and the Antarctic Circumpolar current. In these regions, Chelton et al. (2011)
 62 estimated that coherent eddies contribute around 40–50% of the mesoscale kinetic en-
 63 ergy (Chelton et al., 2011) and thus a significant fraction of the total kinetic energy (Fer-
 64 rari & Wunsch, 2009). Although this unique estimate showcases the importance of the
 65 mesoscale coherent eddy field, the energy contained by coherent eddies was estimated
 66 by extracting the the geostrophic velocities within the detected coherent eddies, thus it
 67 is possible it may contain energy from other processes. Coherent eddies are not only abun-
 68 dant and may have a large proportion of the surface kinetic energy budget, but they also
 69 are essential in the ocean dynamics as concluded by many previous studies (Patel et al.,
 70 2020; Schubert et al., 2019; Pilo et al., 2015; Frenger et al., 2015, 2013; Beron-Vera et
 71 al., 2013; Siegel et al., 2011; Hogg & Blundell, 2006).

72 There is broad consensus that mesoscale eddy kinetic energy has a pronounced sea-
 73 sonal variability (Uchida et al., 2017; Kang & Curchitser, 2017; Qiu & Chen, 2004; Qiu,
 74 1999), several hypothesis proposed to explain this include: seasonal variations of atmo-

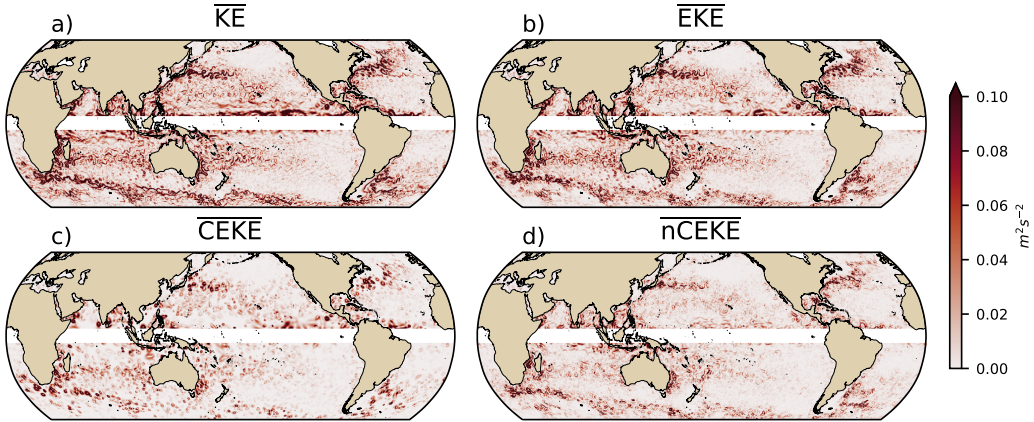
spheric forcing (Sasaki et al., 2014), seasonality of the mixed layer depth (Qiu et al., 2014; Callies et al., 2015), seasonality in the intensity of barotropic instability (Qiu & Chen, 2004), variability of the baroclinic instability due to seasonality of the vertical shear (Qiu, 1999), and a seasonal lag of the inverse energy cascade (energy is transported between scales from small to large; Arbic et al., 2013) in combination with the presence of a front in the mixed layer, which can lead to a seasonal cycle of the baroclinic instability (Qiu et al., 2014). All these factors are likely to influence the seasonal cycle of coherent eddies, however the seasonality of the coherent component of the eddy kinetic energy, as well as the seasonal cycle of the coherent eddy statistics remains unknown.

On one hand, processes such as barotropic and baroclinic instabilities could control the seasonality of coherent eddies in the ocean. On the other hand, recent studies using observations and eddy-permitting climate models suggest several long term adjustments of the global ocean capable of longterm changes in the coherent eddy field. Such readjustments include a multidecadal increase in the ocean stratification resulted from temperature and salinity changes (Li et al., 2020), a horizontal readjusment of the sea surface temperature gradients (Ruela et al., 2020; Bouali et al., 2017; Cane et al., 1997), and a intensification of the kinetic energy, eddy kinetic energy, and mesoscale eddy kinetic energy over the last 3 decades as a consequence of an increase in wind forcing (Hu et al., 2020; Wunsch, 2020; Martínez-Moreno et al., 2021). This global trends readjustments are spatially heterogeneous,

interannual response between wind forcing and the eddy response ()).

an intensification of the ocean forcing and eddy kinetic energy (Martínez-Moreno et al., 2021; Hogg et al., 2015; Hughes & Wilson, 2008) could modify the mesoscale coherent eddy field in decadal timescales.

Here we compute global climatology focusing in the spatial distribution instead of the purely seasonality cycle. The main goal of the present work is to generate a global climatology from the latest satellite observation dataset available, in order to complement the known information of the variability of the superficial Kinetic Energy. The data sources and methodology are described in section 2. Global seasonality, inter-annual variability and trends are explored in sections ??, ??, and ?? respectively. In section ?? we present four regions in which we further investigate the temporal variability of kinetic energy and each of its components.



121 **Figure 1.** Snapshot of surface kinetic energy (\overline{KE}), surface eddy kinetic energy (\overline{EKE}),
122 surface coherent eddy kinetic energy (\overline{CEKE}), and surface non-coherent eddy kinetic energy
123 (\overline{nCEKE}) for the 1st of January 2017.

107 2 Methods

108 2.1 Data

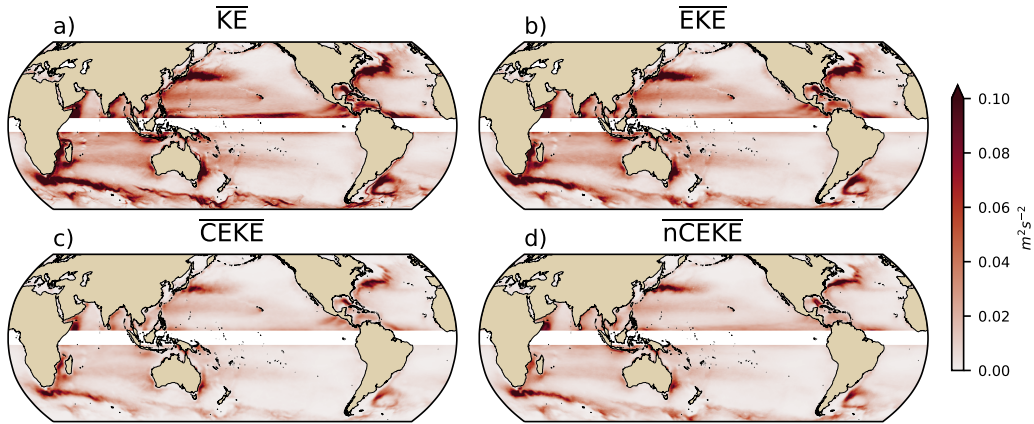
109 2.2 Coherent eddy tracking algorithm

110 2.3 Kinetic Energy decomposition

111 Kinetic energy is commonly divided into the mean and temporal variability com-
112 ponents through a Reynolds decomposition. At a given time, the velocity field (\mathbf{u}) is split
113 into the time mean ($\overline{\mathbf{u}}$) and time varying components (\mathbf{u}'). Additionally, as part of the
114 climatology we also further decompose the eddy kinetic energy into the eddy kinetic en-
115 ergy contained by coherent features (\mathbf{u}'_e) and non-coherent (\mathbf{u}'_n). Therefore the KE equa-
116 tion can be written as:

$$117 \text{KE} = \overline{\mathbf{u}}^2 + \underbrace{\mathbf{u}'_e^2 + \mathbf{u}'_n^2}_{\mathbf{u}'^2} + \mathcal{O}^2 \quad (1)$$

117 The second order terms (\mathcal{O}) are negligible as their time average is two orders of mag-
118 nitude smaller than any other term. For more information about the decomposition of
119 the field into coherent features and non-coherent features refer to Martínez-Moreno et
120 al. (2019).



133 **Figure 2.** Climatology of surface kinetic energy (\overline{KE}), surface eddy kinetic energy (\overline{EKE}),
 134 surface coherent eddy kinetic energy (\overline{CEKE}), and surface non-coherent eddy kinetic energy
 135 (\overline{nCEKE}) between 1993–2018.

124 3 Results

125 3.1 Coherent Eddy Energetics

126 3.1.1 Global

127 **Figure 1**

- 128 • All KE components have large energy contents in the boundary currents and antarc-
 129 tic circumpolar current.
- 130 • In many cases is the same, but there actually some differences There are several
 131 regions where the coherent component is larger than the non-coherent, we will in-
 132 vestigate these in more detail in section XX.

136 **Figure 2**

- 137 • \overline{EKE} is responsible of almost all the \overline{KE} across the ocean, except for regions with
 138 persistent currents over time, such as the mean boundary current locations, equa-
 139 torial pacific currents and regions in the Antarctic Circumpolar current, where the
 140 EKE explains around 40% of the \overline{KE}
- 141 • \overline{EKE} Explains 80% of \overline{KE} , while \overline{CEKE} is 45% of \overline{EKE} and \overline{nCEKE} is 60% of
 142 \overline{EKE}
- 143 • \overline{CEKE} is large equatorwards from the Kuroshio current and Agulhas current.

- Areas with the largest coherent contribution are located in the South of Australia
144
CEKE and South Atlantic
145
- 146
- nCEKE has a large amount of energy at high latitudes, this could be a consequence
147
of the satellites not resolving the mesoscale coherent eddies.
148
- Global averages of the ratios show \overline{EKE} explains around 78% of the ocean MKE
149
field, while coherent eddies and non coherent eddy features contain 49% and 59%
150
per decade. Note this values don't add to 1 as there are cross terms that contain
151
around XX% of the total energy.
152
- 153

161 *3.1.2 Seasonality*

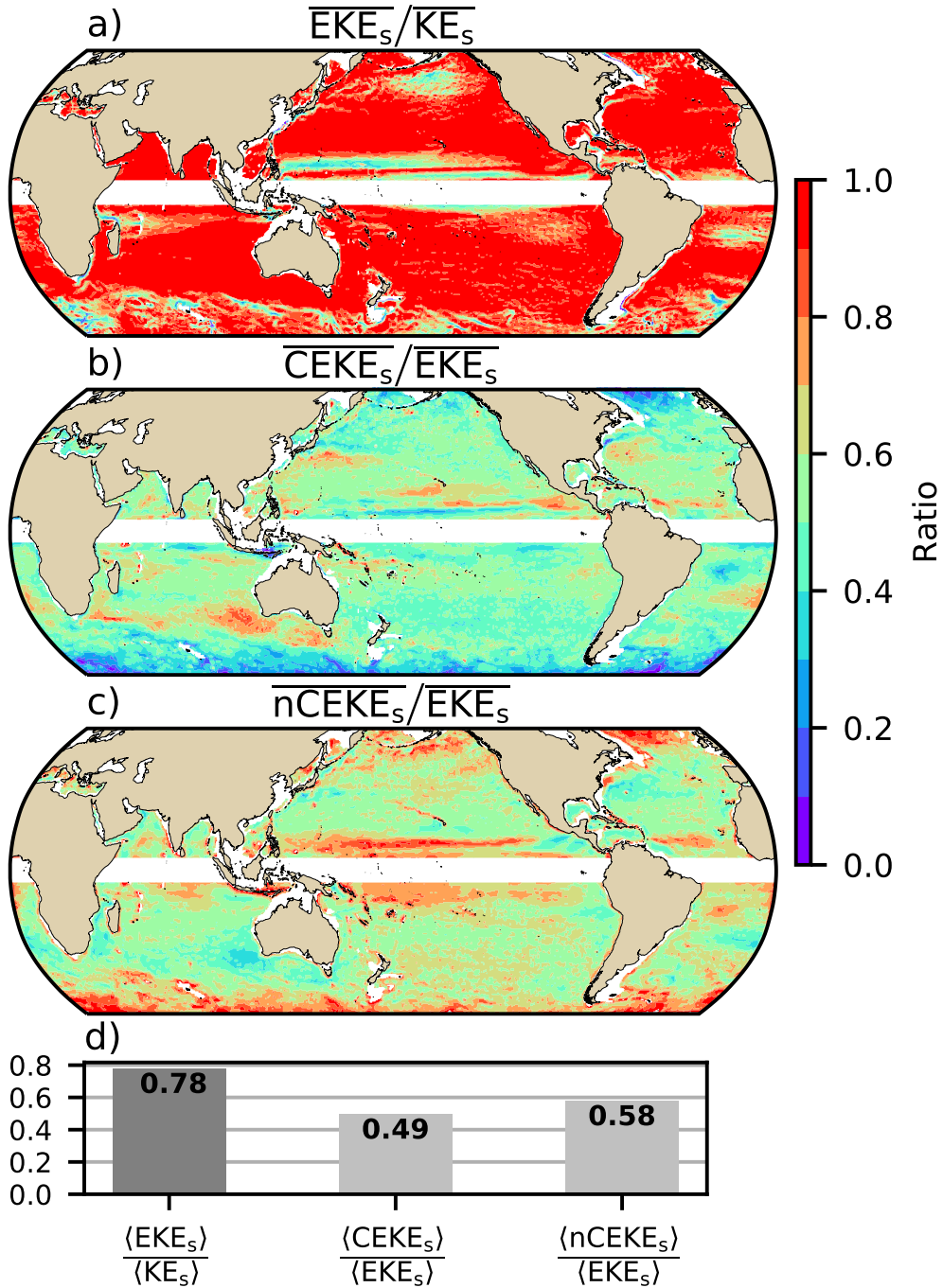
162 **Figure 3**

- The hemisphere seasonality show the EKE and CEKE peak in summer.
163
- Response of the EKE and CEKE show a seasonal lag of \sim 6 months to the forcing
164
of the Winds. Make sure to note the maximum over the hemisphere, locally,
165
the winds may peak in different months.
166
- Methods, explain more about winds or here.
167
- The coherent eddy field show a large interannual variability.
168
- In the Southern Ocean we observe a concentric growth as time passes, which support
169
the increasing trends in the Southern Ocean observed by (Hogg et al., 2015;
170
Martínez-Moreno et al., 2019, 2021)
171
- Point that in the northern hemisphere in winter the CEKE appears to be decreasing.
172
173

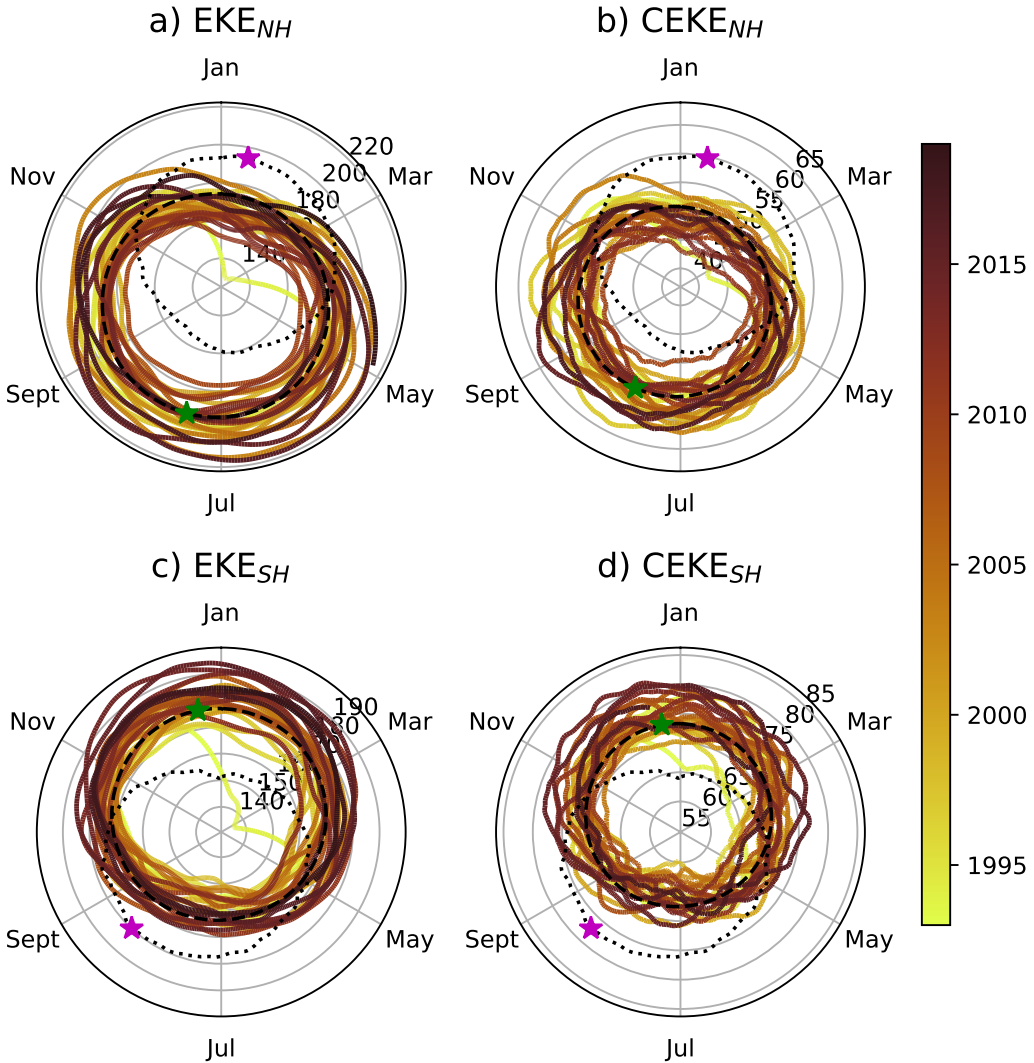
181 **3.2 Coherent Eddy Statistics**

182 *3.2.1 Global*

183 **Figure 4**



154 **Figure 3.** Ratios of the kinetic energy components. a) Map of the proportion of mean eddy
 155 kinetic energy (EKE) versus mean kinetic energy (\overline{KE}); b) Map of the proportion of mean co-
 156 herent eddy kinetic energy (\overline{CEKE}) versus mean eddy kinetic energy (\overline{EKE}); c) Map of the
 157 proportion of mean non-coherent eddy kinetic energy (\overline{nCEKE}) versus mean eddy kinetic energy
 158 (\overline{EKE}); d) Global ratios of mean eddy kinetic energy ($\langle \overline{EKE} \rangle$), mean coherent eddy kinetic en-
 159 ergy ($\langle \overline{CEKE} \rangle$) and mean non coherent eddy kinetic energy ($\langle \overline{nCEKE} \rangle$) versus the global mean
 160 kinetic energy ($\langle \overline{KE} \rangle$) and global mean eddy kinetic energy ($\langle \overline{EKE} \rangle$).



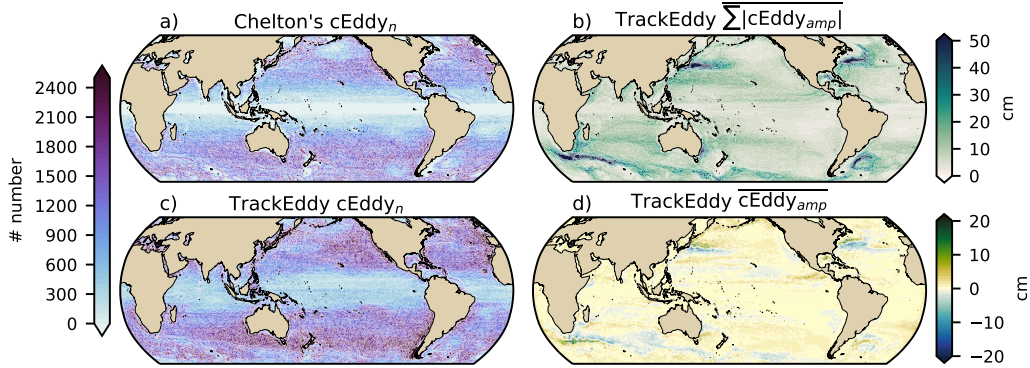
174 **Figure 4. Fix labels** Hemispherical seasonality of eddy kinetic energy (EKE), coherent eddy
 175 kinetic energy (CEKE), and non-coherent eddy kinetic energy (CEKE). Panels a,b and c show
 176 the northern hemisphere seasonal cycle, while panels d,e, and f correspond to the southern hemi-
 177 sphere. Dashed lines correspond to the seasonal climatology of the fields and dotted lines show
 178 the climatology of the wind magnitude. The green and magenta stars show the maximum of the
 179 seasonal cycle for the kinetic energy components and the wind magnitude, respectively. The line
 180 colors show the year.

- A comparison with previous identified numbers show a consistent pattern in the eddy count. The difference in the magnitude could be a consequence of Chelton et al. (2007) filtering the coherent eddies with lifespans longer than 16 weeks.
- Both datasets show a large number of eddies in the East North Pacific, East North Atlantic, as well as the East South Pacific, East South Atlantic and East Indian Ocean.
- While the number of eddies detected in the tropics is quite small.
- Furthermore, there are hotspots of numbers of eddies in other regions of the ocean, such as boundary currents and the Antarctic Circumpolar Current.
- An interesting feature shown in both datasets is a predominant patchiness where the count of the eddies is much larger. These puzzling pattern remains unknown. Although it looks like a propagation pattern, it could be that eddies persist for longer in those areas.
- The eddy amplitude as expected is maximum at the boundary currents and hotspots in the southern ocean.
- Interior of the gyres we can observe that there is an important amplitude of the coherent eddy field.
- Preferred eddy amplitude sign in boundary currents; positive amplitude polewards to the boundary current mean location, and negative amplitude equatorwards. This is consistent with the shed of coherent eddies from the boundary currents.
- There regions with large CEKE ratio show also a large coherent eddy amplitude.

3.2.2 Seasonality

Figure 5

- Seasonality of the number of eddies in the Northern Hemisphere peaks on May, while the Southern Hemisphere peaks on October.
- The seasonality of the amplitude of the eddies is consistent with those of the Coherent eddy kinetic energy.
- Interestingly, there is a 3 month lag between the winds and the seasonality of the number of eddies, while the eddy amplitude responds approximately 6 months after the maximum winds.
- Note that both coherent eddy amplitudes seem to peak around the same time.



205 **Figure 5.** Climatology of the coherent eddy statistics. a) Climatology of the number of coherent
 206 eddies ($cEddy_n$) identified by Chelton et al. (2007); b) Climatology of the warm core coherent
 207 eddy amplitude ($cEddy_{amp}$). c) Climatology of the number of coherent eddies ($cEddy_n$) identi-
 208 fied by Martínez-Moreno et al. (2019); d) Climatology of the cold core coherent eddy amplitude
 209 ($cEddy_{amp}$).

- 220 • If we look closely, the growing-shrinking concentric circles correspond to an increasing-
 221 decreasing trend. These are particularly obvious as a decrease in the eddy num-
 222 ber in the Southern Hemisphere, and a increase in the eddy amplitude.

232 **3.3 Regional**

233 **Figure 6**

- 234 • a

243 **Figure 7**

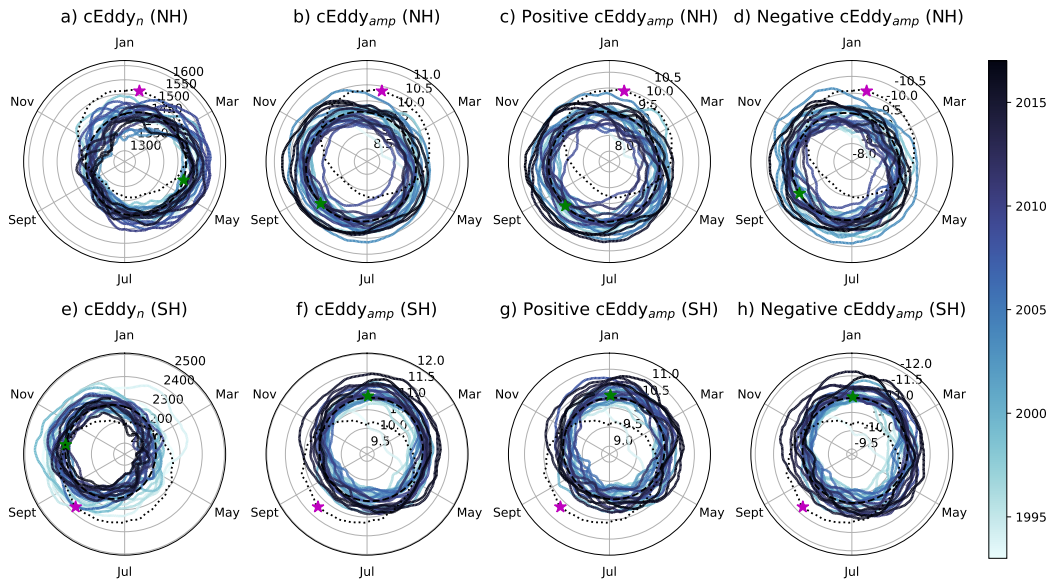
- 244 • a

254 **Figure 8**

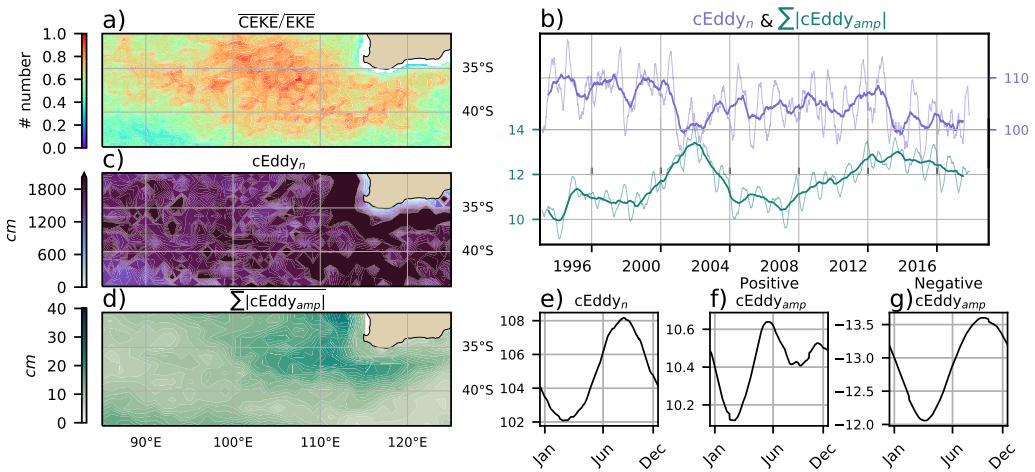
- 255 • a

265 **Figure 9**

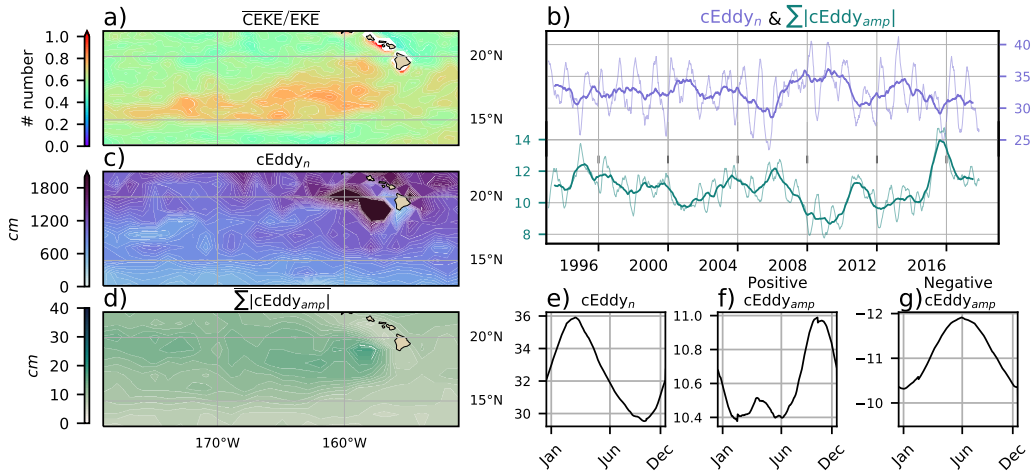
- 266 • a



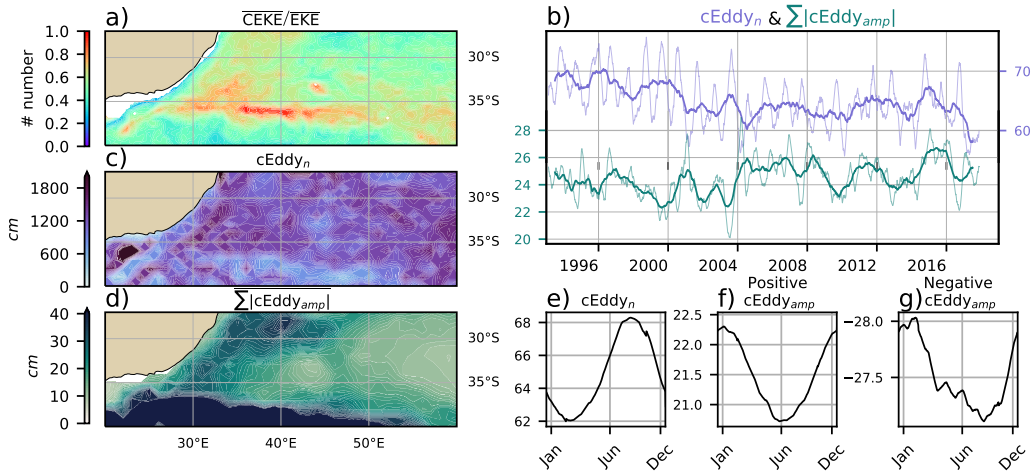
223 **Figure 6.** Hemispherical seasonality of the coherent eddy statistics; a,e) seasonal cycle of the
 224 number of coherent eddies ($cEddy_n$); b,f) seasonal cycle of the mean coherent eddy amplitude
 225 ($cEddy_{amp}$); c,g) seasonal cycle of the warm core coherent eddies amplitude ($wcEddy_{amp}$); d,h)
 226 seasonal cycle of the cold core coherent eddies amplitude ($ccEddy_{amp}$). Panels a,b and c show
 227 the northern hemisphere seasonal cycle, while panels d,e, and f correspond to the southern hemi-
 228 sphere. Dashed lines correspond to the seasonal climatology of the fields and dotted lines show
 229 the climatology of the wind magnitude. The green and magenta stars show the maximum of the
 230 seasonal cycle for the kinetic energy components and the wind magnitude, respectively. The line
 231 colors show the year.



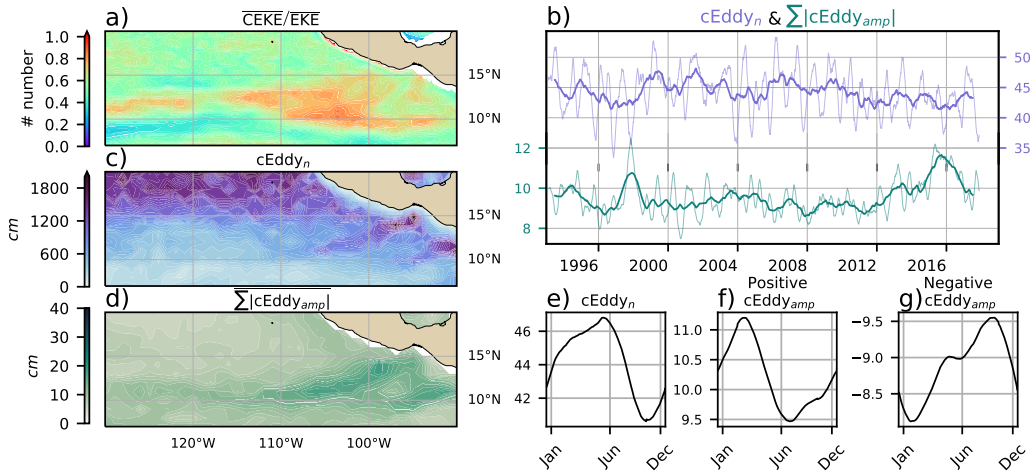
235 **Figure 7.** Climatology of the eddy field and coherent eddy field for the East Indian Ocean. a)
 236 Ratio of mean coherent eddy kinetic energy ($\overline{\text{CEKE}}$) versus mean eddy kinetic energy ($\overline{\text{EKE}}$); b)
 237 Running average over 10 years of the coherent eddy number and amplitude; c) Seasonal cycle of
 238 the number of eddies; d) Map of the number of eddies; e) Multi decadal oscillation of the coher-
 239 ent eddy number; f) Seasonal cycle of the warm core eddies; g) Map of the sum of the absolute
 240 coherent eddy amplitudes; h) Multi decadal oscillation of the coherent eddy number; h) Seasonal
 241 cycle of the cold core eddies. Multi decadal oscillations are defined as the difference between a 2
 242 year running average and a 10 year running average; f) Seasonal cycle of the warm core eddies.



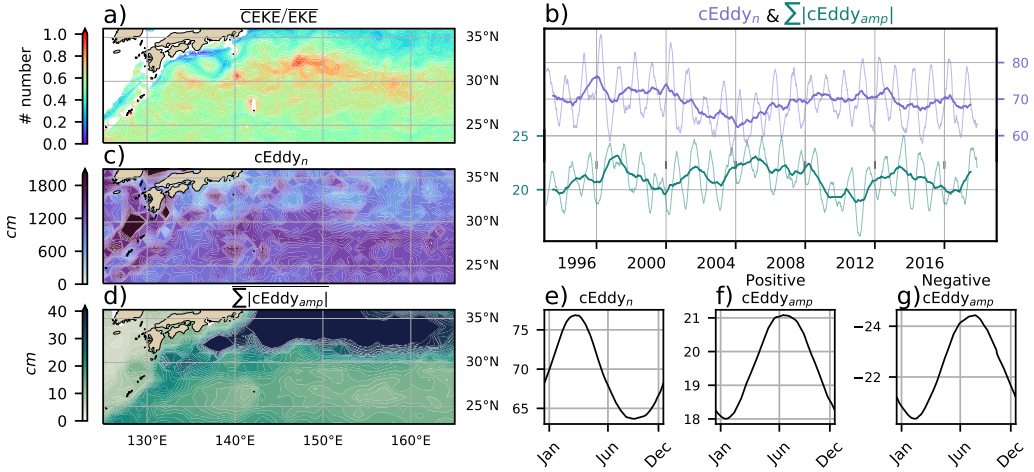
245 **Figure 8.** Climatology of the eddy field and coherent eddy field for the central north pacific.
 246 a) Ratio of mean coherent eddy kinetic energy ($\overline{CEKE}/\overline{EKE}$) versus mean eddy kinetic energy (\overline{EKE});
 247 b) Running average over 10 years of the coherent eddy number and amplitude; c) Seasonal cy-
 248 cle of the number of eddies; d) Map of the number of eddies; e) Multi decadal oscillation of the
 249 coherent eddy number; f) Seasonal cycle of the warm core eddies; g) Map of the sum of the ab-
 250 solute coherent eddy amplitudes; h) Multi decadal oscillation of the coherent eddy number; h)
 251 Seasonal cycle of the cold core eddies. Multi decadal oscillations are defined as the difference
 252 between a 2 year running average and a 10 year running average; f) Seasonal cycle of the warm
 253 core eddies.



256 **Figure 9.** Climatology of the eddy field and coherent eddy field for the Agulhas retroflexion.
 257 a) Ratio of mean coherent eddy kinetic energy (\overline{CEKE}) versus mean eddy kinetic energy (\overline{EKE});
 258 b) Running average over 10 years of the coherent eddy number and amplitude; c) Seasonal cy-
 259 cle of the number of eddies; d) Map of the number of eddies; e) Multi decadal oscillation of the
 260 coherent eddy number; f) Seasonal cycle of the warm core eddies; g) Map of the sum of the ab-
 261 solute coherent eddy amplitudes; h) Multi decadal oscillation of the coherent eddy number; h)
 262 Seasonal cycle of the cold core eddies. Multi decadal oscillations are defined as the difference
 263 between a 2 year running average and a 10 year running average; f) Seasonal cycle of the warm
 264 core eddies.



267 **Figure 10.** Climatology of the eddy field and coherent eddy field for the east tropical pacific.
 268 a) Ratio of mean coherent eddy kinetic energy (\overline{CEKE}) versus mean eddy kinetic energy (\overline{EKE});
 269 b) Running average over 10 years of the coherent eddy number and amplitude; c) Seasonal cy-
 270 cle of the number of eddies; d) Map of the number of eddies; e) Multi decadal oscillation of the
 271 coherent eddy number; f) Seasonal cycle of the warm core eddies; g) Map of the sum of the ab-
 272 solute coherent eddy amplitudes; h) Multi decadal oscillation of the coherent eddy number; h)
 273 Seasonal cycle of the cold core eddies. Multi decadal oscillations are defined as the difference
 274 between a 2 year running average and a 10 year running average; f) Seasonal cycle of the warm
 275 core eddies.



278 **Figure 11.** Climatology of the eddy field and coherent eddy field for the east tropical pacific.
 279
 280 a) Ratio of mean coherent eddy kinetic energy ($\overline{\text{CEKE}}$) versus mean eddy kinetic energy ($\overline{\text{EKE}}$);
 281 b) Running average over 10 years of the coherent eddy number and amplitude; c) Seasonal cy-
 282 cle of the number of eddies; d) Map of the number of eddies; e) Multi decadal oscillation of the
 283 coherent eddy number; f) Seasonal cycle of the warm core eddies; g) Map of the sum of the ab-
 284 solute coherent eddy amplitudes; h) Multi decadal oscillation of the coherent eddy number; h)
 285 Seasonal cycle of the cold core eddies. Multi decadal oscillations are defined as the difference
 286 between a 2 year running average and a 10 year running average; f) Seasonal cycle of the warm
 core eddies.

276 **Figure 10**

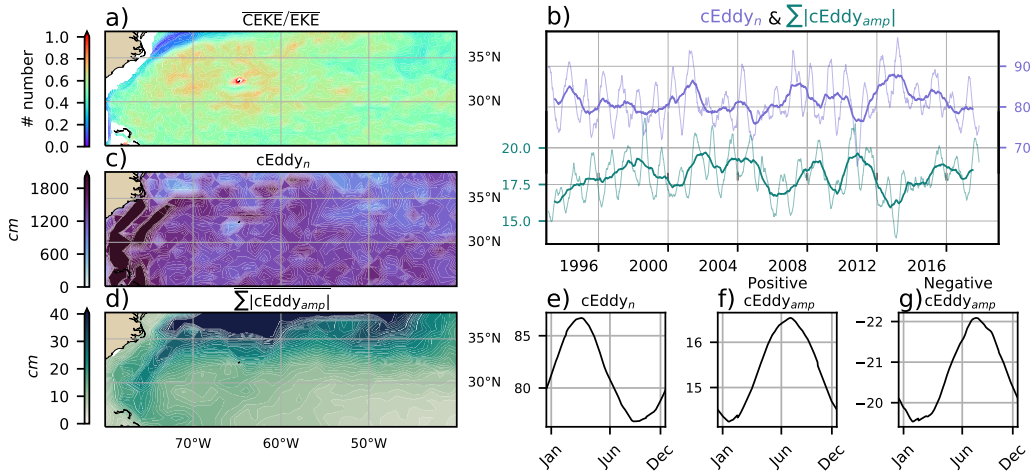
277 • a

287 **Figure 11**

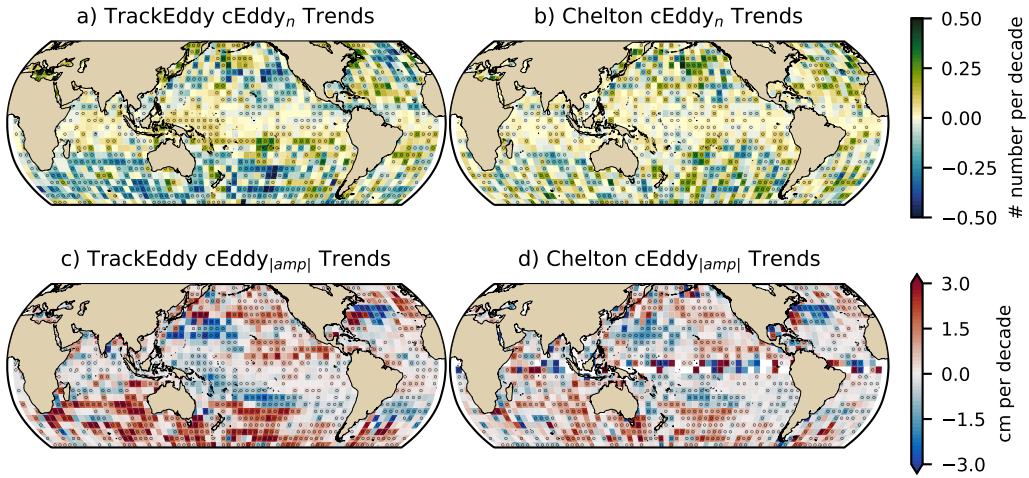
288 • a

289 Should we add the interannual variability of Chelton's?

290 Overall, we observe a polewards decrease in the number of the eddies. This sup-
 291 ports the idea that the satellite observations are consistent with a continue dataset.



289 **Figure 12.** Climatology of the eddy field and coherent eddy field for the east tropical pacific.
 290 a) Ratio of mean coherent eddy kinetic energy ($\overline{CEKE}/\overline{EKE}$) versus mean eddy kinetic energy (\overline{EKE});
 291 b) Running average over 10 years of the coherent eddy number and amplitude; c) Seasonal cy-
 292 cle of the number of eddies; d) Map of the number of eddies; e) Multi decadal oscillation of the
 293 coherent eddy number; f) Seasonal cycle of the warm core eddies; g) Map of the sum of the ab-
 294 solute coherent eddy amplitudes; h) Multi decadal oscillation of the coherent eddy number; h)
 295 Seasonal cycle of the cold core eddies. Multi decadal oscillations are defined as the difference
 296 between a 2 year running average and a 10 year running average; f) Seasonal cycle of the warm
 297 core eddies.



312 **Figure 13.** Trends of coherent eddy statistics. a,b and c Trends of the number of identified
 313 coherent eddies from satellite observations identified using TrackEddy, satellite observations iden-
 314 tified using Chelton's, and state of the art numerical simulation identified using TrackEddy. d,e
 315 and f Trends of the sum of the absolute value of identified coherent eddies amplitude from satel-
 316 lite observations identified using TrackEddy, satellite observations identified using Chelton's, and
 317 state of the art numerical simulation identified using TrackEddy. Gray stippling shows regions
 318 that are statistically significant above the 95% confidence level.

301 4 Trends

302 **Figure 12**

- 303 • The number and amplitude of coherent eddies from two eddy tracking algorithms
 304 show consistent trend patterns.
- 305 • In particular, we observe a decrease in the number of eddies in the southern ocean,
 306 as well as sectors in the North Atlantic and North Pacific.
- 307 • Meanwhile the amplitude seems to be increasing in those same regions.
- 308 • Some of these regions have undergone a readjustment to stronger winds, thus the
 309 observed trends in the eddy amplitude suggests an intensification of the coherent
 310 eddy field to an increase in the forcing.
- 311 • This increase is consistent with Martínez-Moreno et al. (2021)

319 **5 Summary and Conclusions**

320 **Acknowledgments**

321 **References**

- 322 Arbic, B. K., Polzin, K. L., Scott, R. B., Richman, J. G., & Shriver, J. F. (2013).
 323 On Eddy Viscosity, Energy Cascades, and the Horizontal Resolution of Gridded
 324 Satellite Altimeter Products*. *Journal of Physical Oceanography*, *43*(2), 283–300.
 325 doi: 10.1175/jpo-d-11-0240.1
- 326 Ashkezari, M. D., Hill, C. N., Follett, C. N., Forget, G., & Follows, M. J. (2016).
 327 Oceanic eddy detection and lifetime forecast using machine learning methods.
 328 *Geophysical Research Letters*, *43*(23). doi: 10.1002/2016gl071269
- 329 Beron-Vera, F. J., Wang, Y., Olascoaga, M. J., Goni, G. J., & Haller, G. (2013). Ob-
 330 jective Detection of Oceanic Eddies and the Agulhas Leakage. *Journal of Physical*
 331 *Oceanography*, *43*(7), 1426–1438. doi: 10.1175/JPO-D-12-0171.1
- 332 Bouali, M., Sato, O. T., & Polito, P. S. (2017). Temporal trends in sea surface tem-
 333 perature gradients in the South Atlantic Ocean. *Remote Sensing of Environment*,
 334 *194*, 100–114. doi: 10.1016/j.rse.2017.03.008
- 335 Callies, J., Flierl, G., Ferrari, R., & Fox-Kemper, B. (2015). The role of mixed-layer
 336 instabilities in submesoscale turbulence. *Journal of Fluid Mechanics*, *788*, 5–41.
 337 doi: 10.1017/jfm.2015.700
- 338 Cane, M. A., Clement, A. C., Kaplan, A., Kushnir, Y., Pozdnyakov, D., Seager, R.,
 339 ... Murtugudde, R. (1997). Twentieth-Century Sea Surface Temperature Trends.
 340 *Science*, *275*(5302), 957–960. doi: 10.1126/science.275.5302.957
- 341 Chelton, D. B., Gaube, P., Schlax, M. G., Early, J. J., & Samelson, R. M. (2011).
 342 The influence of nonlinear mesoscale eddies on near-surface oceanic chlorophyll.
 343 *Science*, *334*(6054), 328-32. doi: 10.1126/science.1208897
- 344 Chelton, D. B., Schlax, M. G., Samelson, R. M., & de Szoeke, R. A. (2007). Global
 345 observations of large oceanic eddies. *Geophysical Research Letters*, *34*(15),
 346 L15606. doi: 10.1029/2007GL030812
- 347 Cui, W., Wang, W., Zhang, J., & Yang, J. (2020). Identification and census statis-
 348 tics of multicore eddies based on sea surface height data in global oceans. *Acta*
 349 *Oceanologica Sinica*, *39*(1), 41–51. doi: 10.1007/s13131-019-1519-y

- 350 Faghmous, J. H., Frenger, I., Yao, Y., Warmka, R., Lindell, A., & Kumar, V. (2015,
 351 6). A daily global mesoscale ocean eddy dataset from satellite altimetry. *Scientific
 352 Data*, 2, 150028 EP -. doi: 10.1038/sdata.2015.28
- 353 Ferrari, R., & Wunsch, C. (2009). Ocean Circulation Kinetic Energy: Reservoirs,
 354 Sources, and Sinks. *Annual Review of Fluid Mechanics*, 41(1), 253–282. doi: 10
 355 .1146/annurev.fluid.40.111406.102139
- 356 Frenger, I., Gruber, N., Knutti, R., & Münnich, M. (2013). Imprint of Southern
 357 Ocean eddies on winds, clouds and rainfall. *Nature Geoscience*, 6(8), 608 EP -.
 358 doi: 10.1038/ngeo1863
- 359 Frenger, I., Münnich, M., Gruber, N., & Knutti, R. (2015). Southern Ocean eddy
 360 phenomenology. *Journal of Geophysical Research: Oceans*, 120(11), 7413-7449.
 361 doi: 10.1002/2015JC011047
- 362 Fu, L., Chelton, D., Le Traon, P., & Oceanography, M. R. (2010). Eddy dynamics
 363 from satellite altimetry. *Oceanography*, 23(4), 14-25. doi: 10.2307/24860859
- 364 Gill, A., Green, J., & Simmons, A. (1974). Energy partition in the large-scale ocean
 365 circulation and the production of mid-ocean eddies. *Deep Sea Res Oceanogr Abstr*,
 366 21(7), 499-528. doi: 10.1016/0011-7471(74)90010-2
- 367 Hogg, A. M., & Blundell, J. R. (2006). Interdecadal variability of the southern
 368 ocean. *Journal of Physical Oceanography*, 36(8), 1626-1645. doi: 10.1175/
 369 JPO2934.1
- 370 Hogg, A. M., Meredith, M. P., Chambers, D. P., Abrahamsen, E. P., Hughes,
 371 C. W., & Morrison, A. K. (2015). Recent trends in the Southern Ocean
 372 eddy field. *Journal of Geophysical Research: Oceans*, 120(1), 257-267. doi:
 373 10.1002/2014JC010470
- 374 Hu, S., Sprintall, J., Guan, C., McPhaden, M. J., Wang, F., Hu, D., & Cai,
 375 W. (2020, 2). Deep-reaching acceleration of global mean ocean circula-
 376 tion over the past two decades. *Science Advances*, 6(6), eaax7727. doi:
 377 10.1126/sciadv.aax7727
- 378 Hughes, C. W., & Wilson, C. (2008). Wind work on the geostrophic ocean cir-
 379 culation: An observational study of the effect of small scales in the wind stress.
 380 *Journal of Geophysical Research: Oceans (1978–2012)*, 113(C2), C02016. doi:
 381 10.1029/2007JC004371
- 382 Kang, D., & Curchitser, E. N. (2017). On the Evaluation of Seasonal Variability of

- 383 the Ocean Kinetic Energy. *Geophysical Research Letters*, 47, 1675–1583. doi: 10
384 .1175/JPO-D-17-0063.1
- 385 Li, G., Cheng, L., Zhu, J., Trenberth, K. E., Mann, M. E., & Abraham, J. P. (2020).
386 Increasing ocean stratification over the past half-century. *Nature Climate Change*,
387 1–8. doi: 10.1038/s41558-020-00918-2
- 388 Martínez-Moreno, J., Hogg, A. M., England, M., Constantinou, N. C., Kiss, A. E.,
389 & Morrison, A. K. (2021). Global changes in oceanic mesoscale currents over the
390 satellite altimetry record. *Journal of Advances in Modeling Earth Systems*, 0(ja).
391 doi: 10.1029/2019MS001769
- 392 Martínez-Moreno, J., Hogg, A. M., Kiss, A. E., Constantinou, N. C., & Mor-
393 rison, A. K. (2019). Kinetic energy of eddy-like features from sea surface
394 altimetry. *Journal of Advances in Modeling Earth Systems*, 0(ja). doi:
395 10.1029/2019MS001769
- 396 Patel, R. S., Llort, J., Strutton, P. G., Phillips, H. E., Moreau, S., Pardo, P. C.,
397 & Lenton, A. (2020). The Biogeochemical Structure of Southern Ocean
398 Mesoscale Eddies. *Journal of Geophysical Research: Oceans*, 125(8). doi:
399 10.1029/2020jc016115
- 400 Pilo, G. S., Mata, M. M., & Azevedo, J. L. L. (2015). Eddy surface properties and
401 propagation at Southern Hemisphere western boundary current systems. *Ocean
402 Science*, 11(4), 629–641. doi: 10.5194/os-11-629-2015
- 403 Qiu, B. (1999). Seasonal Eddy Field Modulation of the North Pacific Subtropical
404 Countercurrent: TOPEX/Poseidon Observations and Theory. *Journal of Physical
405 Oceanography*, 29(10), 2471–2486. doi: 10.1175/1520-0485(1999)029<2471:sefmot>2
406 .0.co;2
- 407 Qiu, B., & Chen, S. (2004). Seasonal Modulations in the Eddy Field of the South
408 Pacific Ocean. *Journal of Physical Oceanography*, 34(7), 1515–1527. doi: 10.1175/
409 1520-0485(2004)034<1515:smitef>2.0.co;2
- 410 Qiu, B., Chen, S., Klein, P., Sasaki, H., & Sasai, Y. (2014). Seasonal Mesoscale
411 and Submesoscale Eddy Variability along the North Pacific Subtropical Coun-
412 tercurrent. *Journal of Physical Oceanography*, 44(12), 3079–3098. doi:
413 10.1175/jpo-d-14-0071.1
- 414 Ruela, R., Sousa, M. C., deCastro, M., & Dias, J. M. (2020). Global and regional
415 evolution of sea surface temperature under climate change. *Global and Planetary*

- 416 *Change*, 190, 103190. doi: 10.1016/j.gloplacha.2020.103190
- 417 Sasaki, H., Klein, P., Qiu, B., & Sasai, Y. (2014). Impact of oceanic-scale inter-
418 actions on the seasonal modulation of ocean dynamics by the atmosphere. *Nature
419 Communications*, 5(1), 5636. doi: 10.1038/ncomms6636
- 420 Schubert, R., Schwarzkopf, F. U., Baschek, B., & Biastoch, A. (2019). Submesoscale
421 Impacts on Mesoscale Agulhas Dynamics. *Journal of Advances in Modeling Earth
422 Systems*, 11(8), 2745–2767. doi: 10.1029/2019ms001724
- 423 Siegel, D., Peterson, P., DJ, M., Maritorena, S., & Nelson, N. (2011). Bio-optical
424 footprints created by mesoscale eddies in the Sargasso Sea. *Geophysical Research
425 Letters*, 38(13), n/a-n/a. doi: 10.1029/2011GL047660
- 426 Uchida, T., Abernathey, R., & Smith, S. (2017). Seasonality of eddy kinetic energy
427 in an eddy permitting global climate model. *Ocean Modelling*, 118, 41-58. doi: 10
428 .1016/j.ocemod.2017.08.006
- 429 Wunsch, C. (2020). Is The Ocean Speeding Up? Ocean Surface Energy Trends.
430 *Journal of Physical Oceanography*, 50(11), 1–45. doi: 10.1175/jpo-d-20-0082.1
- 431 Wunsch, C., & Ferrari, R. (2004). VERTICAL MIXING, ENERGY, AND THE
432 GENERAL CIRCULATION OF THE OCEANS. *Annual Review of Fluid Me-
433 chanics*, 36(1), 281–314. doi: 10.1146/annurev.fluid.36.050802.122121
- 434 Wyrtki, K., Magaard, L., & Hager, J. (1976). Eddy energy in the oceans. *Journal of
435 Geophysical Research*, 81(15), 2641-2646. doi: 10.1029/JC081i015p02641